STABILITY OF THE **G**-MATRIX IN A POPULATION EXPERIENCING PLEIOTROPIC MUTATION, STABILIZING SELECTION, AND GENETIC DRIFT

ADAM G. JONES,[1,2] STEVAN J. ARNOLD,[3] AND REINHARD BÜRGER[4]

[1]*School of Biology, 310 Ferst Drive, Georgia Institute of Technology, Atlanta, Georgia 30332*
[2]*E-mail: adam.jones@biology.gatech.edu*
[3]*Department of Zoology, 3029 Cordley Hall, Oregon State University, Corvallis, Oregon 97331*
[4]*Institut für Mathematik, Universität Wien, A-1090 Wien, Austria*

Abstract.—Quantitative genetics theory provides a framework that predicts the effects of selection on a phenotype consisting of a suite of complex traits. However, the ability of existing theory to reconstruct the history of selection or to predict the future trajectory of evolution depends upon the evolutionary dynamics of the genetic variance-covariance matrix (**G**-matrix). Thus, the central focus of the emerging field of comparative quantitative genetics is the evolution of the **G**-matrix. Existing analytical theory reveals little about the dynamics of **G**, because the problem is too complex to be mathematically tractable. As a first step toward a predictive theory of **G**-matrix evolution, our goal was to use stochastic computer models to investigate factors that might contribute to the stability of **G** over evolutionary time. We were concerned with the relatively simple case of two quantitative traits in a population experiencing stabilizing selection, pleiotropic mutation, and random genetic drift. Our results show that **G**-matrix stability is enhanced by strong correlational selection and large effective population size. In addition, the nature of mutations at pleiotropic loci can dramatically influence stability of **G**. In particular, when a mutation at a single locus simultaneously changes the value of the two traits (due to pleiotropy) and these effects are correlated, mutation can generate extreme stability of **G**. Thus, the central message of our study is that the empirical question regarding **G**-matrix stability is not necessarily a general question of whether **G** is stable across various taxonomic levels. Rather, we should expect the **G**-matrix to be extremely stable for some suites of characters and unstable for others over similar spans of evolutionary time.

Key words.—Genetic correlation, genetic covariance, genetic variance, pleiotropy, response to selection, quantitative genetics.

Modern quantitative genetics theory provides points of connection between microevolution and macroevolution (Arnold et al. 2001). For a phenotype comprising multiple traits, the single-generation response to selection is given by the multivariate version of the breeder's equation (Lande 1979), $\Delta\bar{\mathbf{z}} = \mathbf{G}\boldsymbol{\beta}$, where $\bar{\mathbf{z}}$ is a vector of population trait means, $\boldsymbol{\beta}$ is a vector of directional selection gradients, and **G** is the genetic variance-covariance matrix (the **G**-matrix). Hence, the response to selection depends upon the intensity and direction of selection, as well as upon the amount of genetic variation and the nature of genetic correlations among traits. This equation for the change in the mean phenotype can be extrapolated over multiple generations to reconstruct the history of selection or to predict the future trajectory of the phenotype as a consequence of selection. This potential for extrapolation provides a connection between microevolutionary processes and macroevolutionary patterns (Lande 1979; but see Zeng 1988). However, such an extrapolation is possible only if the **G**-matrix remains relatively constant over long spans of evolutionary time. An extremely unstable **G**-matrix would render the goal of understanding selection over evolutionary time unachievable within the existing quantitative genetics theory framework.

Because of the central role of the **G**-matrix in quantitative genetics and the implications of its evolution, **G**-matrix stability has been a major focus of recent studies. In fact, this enterprise has grown so much in size that it is fair to say that a new field of comparative quantitative genetics has arisen (Steppan et al. 2002), whose primary purview is the evolution of the **G**-matrix itself. However, despite several decades of work, how the **G**-matrix changes over evolutionary

time remains a major unresolved issue. Neither empirical nor theoretical investigations have led to a consensus with respect to the expected stability of the **G**-matrix over evolutionary time.

On the empirical side, the study of **G**-matrix evolution has relied upon comparisons of **G**-matrices across distinct populations of organisms. Clearly, over extremely long spans of evolutionary time the **G**-matrix must change appreciably, since among very divergent taxa, dramatic changes in bauplans result in many structures that cannot be equated with one another in a quantitative genetic framework. Over shorter periods of evolutionary time, however, empirical results demonstrate that the **G**-matrix often remains stable. For example, numerous comparisons of **G** between populations within species have revealed **G**-matrix equality (Billington et al. 1988; Shaw and Billington 1991; Spitze et al. 1991; Platenkamp and Shaw 1992; Brodie 1993; Podolsky et al. 1997; Service 2000). Other studies have shown that **G**-matrices may vary somewhat between populations while still retaining evolutionarily important aspects of their structure (Arnold and Phillips 1999; Roff and Mousseau 1999). Stability or conservation of structure has even been demonstrated for some comparisons between species within genera (Roff et al. 1999; Begin and Roff 2001). However, enough studies have demonstrated **G**-matrix inequality that we cannot tacitly assume that the **G**-matrix remains constant over long spans of time. Instability of **G** is particularly obvious in comparisons among species or among genera (Kohn and Atchley 1988; Paulsen 1996; Waldmann 2000), but **G** has also been shown to vary in response to genetic drift and environmental perturbations

(Shaw et al. 1995; Guntrip et al. 1997; Begin and Roff 2001; Phillips et al. 2001).

Existing theory on the evolution of the **G**-matrix produces conclusions similar to those that can be drawn from the empirical studies: some conditions are expected to produce stability, while others are not. Turelli (1988) outlined several conditions that may promote **G**-matrix constancy, including: (1) no genotype-by-environment interaction with respect to the values of genetic variances and covariances; (2) no direct change in the nature of environmental effects on the phenotype over time; (3) a constant curvature and orientation of the adaptive landscape (even though the optimum can change); and (4) no change in the nature of genetic covariances associated with new mutations. In addition, the number of loci, number of alleles per locus, and the distribution of allelic effects can be important to the stability of **G** (Turelli 1988). Furthermore, linkage disequilibrium during periods of strong, fluctuating selection can induce transient changes in the **G**-matrix, a phenomenon referred to as the ''Bulmer effect'' (Bulmer 1980; Turelli 1988; Shaw et al. 1995). Overall, these theoretical considerations have fostered a grim outlook on the prospects of long-term stability of **G**, with some authors suggesting that the **G**-matrix is not useful over evolutionary time scales. Nevertheless, the current state of analytical theory on **G**-matrix evolution is that existing theory cannot guarantee stability of the **G**-matrix (Turelli 1988), but also does not guarantee instability. In fact, existing theory provides very little information with respect to how much **G** will change as a result of violations of the criteria for stability laid out by Turelli (1988). Consequently, we are left to wonder if the changes in **G**-matrix structure that seem likely based on theoretical considerations are of sufficient magnitude to affect evolutionary inferences.

Due to the complexity of the problem, analytical theory appears to have reached an impasse with respect to further progress on the issue of **G**-matrix stability, but a hitherto unexplored approach is to use stochastic simulations to investigate this important topic. Such a modeling approach has led to useful insights in quantitative genetic studies involving single traits. For example, stochastic models have been used to address the maintenance of genetic variance for quantitative traits in finite populations (Bulmer 1972; Barton 1989; Bürger et al. 1989; Keightley and Hill 1989; Foley 1992; Bürger and Lande 1994) and the risk of extinction due to quantitative trait evolution in response to environmental change (Bürger and Lynch 1995). So far, few studies have attempted to extend these stochastic models to problems involving a phenotype comprising multiple traits (Wagner 1989; Baatz and Wagner 1997; Wagner et al. 1997; Reeve 2000), and none has investigated the stability of **G** in detail. Hence, our aim in the present study is to extend these stochastic models to investigate the factors that influence **G**-matrix stability.

As a first step in developing stochastic models of the **G**-matrix, we address the situation in which a finite population is subject to stabilizing selection and mutation. Our specific goals are to investigate the relative roles of effective population size, the shape of the adaptive landscape, and the nature of mutational parameters on the **G**-matrix over thousands of generations of evolution. The essential features of the **G**-matrix can be illustrated by using a phenotype composed of two quantitative traits, so we restrict our attention in this initial study to a situation in which two traits are determined by a suite of pleiotropic loci. The results of this analysis are relevant to debates regarding the stability of the **G**-matrix, and they pinpoint certain parameters of fundamental importance to the genetic architecture of the multivariate phenotype.

METHODS

The Simulation Model

The simulation model used in this study is a direct extension of that employed by Bürger et al. (1989) and Bürger and Lande (1994). We used Monte Carlo simulations, with an additive genetic model in which all loci in all individuals were explicitly modeled. The extension of the univariate model to two traits resulted in numerous additional parameters, so for those parameters that were investigated in the single-trait simulations, we chose parameter values that seemed reasonable from those earlier studies (Bürger and Lande 1994). The two traits in our model were determined by n unlinked loci, all of which were pleiotropic. This situation can result in a genetic correlation between the two traits, but it need not do so, depending on the nature of mutational effects and selection. A mutation at a locus resulted in a new allele with new effects on both traits. These effects were drawn from a bivariate Gaussian distribution with means of zero, variances of α_1^2 and α_2^2, and a correlation of r_μ. They then were added to the existing effects of the allele in accord with the continuum of alleles model (Crow and Kimura 1964). We determined an individual's phenotype at each trait by summing across loci and adding environmental variation drawn randomly from a normal distribution with a mean of zero and a variance of one. Environmental effects on multiple traits were uncorrelated.

We simulated a diploid, sexually reproducing population with a constant population size of N. The life cycle consisted of: (1) production of progeny from the previous generation of adults (including mutation); (2) viability selection; and (3) random choice of the new generation of adults from the survivors of selection. We used a monogamous mating system for these simulations, and generations did not overlap. For the parameter combinations that we investigated, selection was relatively weak, such that at least N progeny always survived the viability selection phase of the life cycle. The fitness of each individual was determined by an individual selection surface with the shape of a multivariate Gaussian distribution, such that the fitness of phenotype **z**, $W(\mathbf{z})$, was given by

$$W(\mathbf{z}) = \exp\left[-\frac{1}{2}(\mathbf{z} - \boldsymbol{\theta})^{\mathrm{T}}\boldsymbol{\omega}^{-1}(\mathbf{z} - \boldsymbol{\theta})\right], \qquad (1)$$

where **z** is a column vector of trait values, **θ** is a column vector of trait optima, and the superscript T denotes matrix transposition (Lande 1979). The matrix **ω** describes the curvature and orientation of the individual selection surface. For the two-character case, **ω** contains the elements ω_{11}, ω_{22}, and ω_{12}. The diagonal elements, ω_{11} and ω_{22}, represent the strength of stabilizing selection and are analogous to the var-

iance of the bivariate normal distribution. Thus, larger values of ω_{11} and ω_{22} result in weaker stabilizing selection. The orientation of the selection surface is determined by ω_{12}, which is analogous to the covariance of a bivariate normal distribution.

Each simulation run was preceded by 10,000 generations of stabilizing selection, during which a genetically uniform starting population reached a mutation-selection-drift equilibrium. The following 2000 to 4000 generations were the experimental generations, during which population-level values were calculated every generation. Most notably, we calculated the elements of the **G**-matrix, as well as the genetic and phenotypic means. We also calculated the single-generation change in each population-level variable. In this analysis, we restrict attention to the absolute values of these single-generation changes, because under a stabilizing selection equilibrium there is no net directionality to the changes on average.

Because the mating system was monogamous in our model, with no variance in the number of offspring produced by each female, our effective population size was actually somewhat larger than the census population size. Each breeding pair in our simulation produced exactly $2B$ offspring, and we held B constant at 2. Under these circumstances, the effective population size is $N_e = 4N/(V_k + 2)$, where the variance in family size, V_k, is given by $V_k = 2(1 - 1/B)[1 - (2B - 1)/(BN - 1)]$ (Bürger and Lande 1994). We used census population sizes of 256, 512, 1028, and 2056, which corresponded to effective population sizes of 342, 683, 1366, and 2731, respectively.

Throughout this study, we used the following standard parameters (unless otherwise mentioned): the number of loci contributing to the trait, n, is 50, the mutation rate is $\mu = 0.0002$ per haploid locus, the variances of mutational effects (α_1^2 and α_2^2) are 0.05 for both traits, and the loci are freely recombining. Therefore, the genomic mutation rate is $2n\mu = 0.02$ and for each trait the input of genetic variance due to new mutations per generation is 10^{-3}. With these parameter combinations, V_m/σ_e^2 is also 10^{-3}, a value close to those observed in empirical studies of mutational variance (Lande 1975; Lynch 1988; Lynch and Walsh 1998). Our choice of parameters was governed mainly by the previous results of Bürger and Lande (1994), so the parameter values that we used in our simulations were similar to those that formed the nucleus of this previous simulation-based analysis. Future studies may well benefit from a greater departure from the parameters used by Bürger and Lande (1994), but such analyses are outside the scope of this initial study.

Quantifying **G**-matrix Stability

The most obvious way to study the degree of stability of the size and shape of the **G**-matrix under a balance between multivariate stabilizing selection, pleiotropic mutation, and random genetic drift would be to consider the genetic variances (G_{11}, G_{22}) and the covariance (G_{12}), or correlation (r_g), and how they change during evolution. Another way is to look at the eigenvalues (λ_1, λ_2) of the **G**-matrix, at their ratio (ϵ, defined here as the smaller eigenvalue divided by the larger) as a measure of the shape of the **G**-matrix (thus, ϵ is

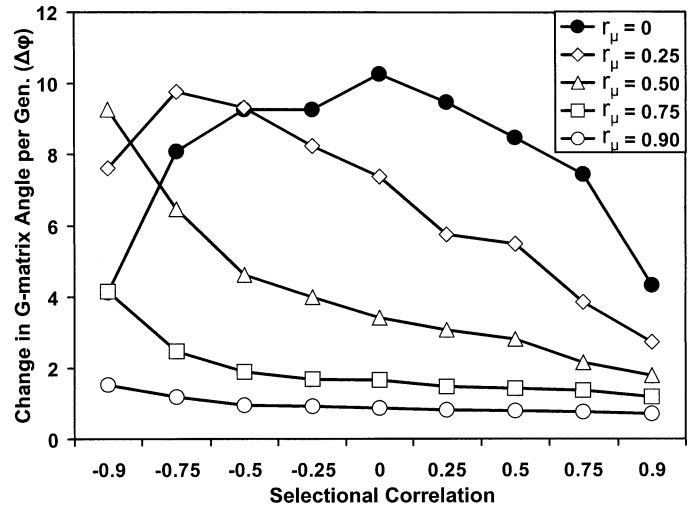
FIG. 1. The combined influence of selectional and mutational correlation on the average between-generation change of the orientation of the **G**-matrix ($\Delta\varphi$). As indicated, each of the five lines displays $\Delta\varphi$ as a function of the selectional correlation r_ω for a given value of r_μ. The following parameters are the same for all panels: $N_e = 342$, $\omega_{11} = \omega_{22} = 49$, $\alpha_1^2 = \alpha_2^2 = 0.05$. See text for other parameter values used in the model.

inversely related to the eccentricity), and at the angle (φ) between the leading eigenvector and the axis along which the first trait is measured (i.e., the x-axis). This angle φ is measured in degrees, ranging from $-90°$ to $+90°$, thus providing a convenient measure for the orientation of the **G**-matrix. Small ϵ means high eccentricity, or as we often shall call it, a cigar-shaped **G**-matrix. As a measure for the overall size of the **G**-matrix we use the total genetic variance, $\Sigma = G_{11} + G_{22}$. Thus, a two-dimensional **G**-matrix is fully described by Σ, ϵ, and φ. Both perspectives, variances and covariance versus size, shape, and orientation yield interesting and complementary insights.

In our tables, we present the average values of the genetic variances of the two traits, their genetic covariance and their correlation. We also present average values of the eigenvalues (λ_1, λ_2), total size (Σ), shape (ϵ), and orientation (φ) of the **G**-matrix. These average values were obtained by averaging over 20 replicate runs, each over 2000 generations (except in the case of Fig. 1, for which values were averaged over 4000 generations), measuring the quantities of interest each generation. This method is a compromise between two alternative methods for obtaining an estimator for the mean of a random variable distributed according to a stationary stochastic process: namely, averaging over a very long time series or averaging over single values from a large number of replicate runs. Because the generation of an initial population in quasi-equilibrium requires much computer time, and because of high temporal autocorrelations within single replicate runs, the adopted method seems to be appropriate (see also Bürger et al. 1989; Bürger and Lande 1994).

As measures for the stability of the size, the shape, and the orientation, we use the average of the absolute values of change between two successive generations and denote them by ΔG_{11}, ΔG_{22}, ΔG_{12}, $\Delta\lambda_1$, $\Delta\lambda_2$, $\Delta\Sigma$, $\Delta\epsilon$, and $\Delta\varphi$. We standardized ΔG_{11}, ΔG_{22}, $\Delta\lambda_1$, $\Delta\lambda_2$, $\Delta\Sigma$, and $\Delta\epsilon$ relative to their

average magnitudes by dividing them by their corresponding mean (i.e., ΔG_{11} is the average single-generation change in the genetic variance for trait 1, divided by the mean genetic variance for trait 1). However, the change of the angle ($\Delta\varphi$) does not require this kind of normalization. In addition, the mean covariance is close to zero for some parameter combinations, so we did not standardize ΔG_{12}. Thus, ΔG_{11}, ΔG_{22}, $\Delta\lambda_1$, $\Delta\lambda_2$, $\Delta\Sigma$, and $\Delta\epsilon$ represent the average between-generation change relative to the mean, whereas $\Delta\varphi$ and ΔG_{12} are simply the average between-generation changes.

The Expected Genetic Variance

For comparison of the dynamics of the genetic variance of our traits determined by pleiotropic loci with those expected of a single, completely independent trait experiencing stabilizing selection, genetic drift, and mutation, we also calculated the stochastic house-of-cards approximation for the expected genetic variance of a single trait (Barton 1989; Bürger et al. 1989; Houle 1989; Keightley and Hill 1989). Under this model, the formula for the expected genetic variance is

$$\hat{\sigma}_g^2(SHC) = \frac{4n\mu\alpha^2 N_e}{1 + (\alpha^2 N_e/V_s)}, \tag{2}$$

where n is the number of loci, μ is the per-locus mutation rate, α^2 is the variance of the distribution of mutational effects, and V_s, the strength of stabilizing selection on breeding values, is equal to the ω corresponding to the trait (i.e., ω_{11} for trait 1) plus the environmental variance (which we are holding constant at one; Bürger and Lande 1994). This formula gives the expected genetic variance for a single trait evolving in complete isolation from other traits. We were interested in comparing these expectations with the equilibrium levels of genetic variation in a trait experiencing stabilizing selection, while genetically associated, through pleiotropy, with a second trait also experiencing stabilizing selection.

RESULTS

Stabilizing Selection and the G-matrix

Table 1 summarizes the effects of variation in the strength of stabilizing selection on the two traits and on their covariance for a population of effective size $N_e = 342$ in the absence of correlation between the mutational effects ($r_\mu = 0$). Table 1 clearly shows that stronger correlational selection (increasing r_ω) decreases the genetic variance of both traits as well as both eigenvalues, hence also decreasing the overall size Σ of the matrix. In parallel, it increases the genetic covariance and correlation between the traits. In addition, in the absence of selectional correlation, asymmetric stabilizing selection ($\omega_{11} \neq \omega_{22}$) has the consequence that stronger selection on the second trait ($\omega_{11} > \omega_{22}$) reduces the variance of this trait to a greater extent than that of the first trait. The variance of the first trait is reduced, too, despite the absence of genetic covariance, because each single mutation has pleiotropic effects on both traits, and only on average do they cancel. The shape measure ϵ decreases with increasing selectional correlation, but not very much, that is, correlational selection promotes eccentricity of the G-matrix to a moderate

extent. The average angle φ does not differ significantly from zero if mutational and selection correlations are both zero ($r_\mu = r_\omega = 0$), but it is highly variable in this case. With increasing r_ω, it quickly increases to nearly 45° if the two traits experience the same strength of stabilizing selection. For asymmetric stabilizing selection, this angle increases to a much smaller degree.

The average between-generation change of the genetic variances and of the overall size is almost unaffected by any change in the selection pattern, reflecting the fact that fluctuations in the variances and the size of the G-matrix are mainly determined by random genetic drift (see Table 2, which shows that ΔG_{11}, ΔG_{22}, and $\Delta\Sigma$ decrease as N_e increases). However, the between-generation change of the major eigenvalue increases with increasing correlational selection, whereas that of the smaller eigenvalue decreases correspondingly. Interestingly, the standardized between-generation change of the shape, $\Delta\epsilon$, is nearly independent of r_ω, although ϵ itself decreases as r_ω increases. In other words, regardless of the value of r_ω, the per-generation change in ϵ is a constant fraction (about 10% for $N_e = 342$) of its mean. However, $\Delta\epsilon$ does depend on N_e (Table 2). By contrast, the between-generation change of the covariance (ΔG_{12}), as well as that of the orientation ($\Delta\varphi$), decreases with increasing r_ω. These patterns reflect the fact that stronger correlational selection causes higher stability in the orientation of the G-matrix, though it has virtually no effect on the stability of the genetic variances, the total size, and the shape.

Interestingly, if one trait is under stronger stabilizing selection than the other, the between-generation change of the angle is reduced below that observed if both traits experience the same strength of selection, weak or strong. This is true for any value of r_ω. The between-generation change of the shape parameter, $\Delta\epsilon$, is remarkably inert to any changes in the strength of selection on the two characters, even to extreme asymmetries. Thus, like correlational selection, asymmetric stabilizing selection promotes orientation stability. Overall, Table 1 shows that the stability properties of the size and shape of a G-matrix depend in a qualitatively similar way on the shape of the fitness landscape. Also, at least in such small populations, the size, shape, and orientation of the G-matrix are rather unstable in the absence of mutational correlation: The average between-generation change of the total size is between 5% and 6% of the mean, that of the shape parameter is about 10% of the mean, and the average between-generation change of the orientation, $\Delta\varphi$, is always at least 3° and reaches nearly 10° in the absence of any correlation (see Fig. 2 for a time series showing the evolution of φ).

The Nature of Mutations and G-matrix Stability

In contrast to stabilizing selection alone, mutational correlation has a much stronger influence on the shape of the G-matrix and its orientation stability. Table 3 summarizes the effects of increasing the mutational correlation for different strengths of stabilizing selection on the two traits in the absence of correlational selection. First, increasing r_μ has only a slight negative effect on the average genetic variances (or even none for G_{22} in the case of unequal selection

TABLE 1. The influence of the orientation and curvature of the adaptive landscape on G-matrix stability during stabilizing selection. The following parameters are fixed: N_e = 342, r_μ = 0, $\alpha_1^2 = \alpha_2^2 = 0.05$. See text for other parameter values, the definitions of symbols, and the methods by which these mean values were calculated. The values of ΔG_{11}, ΔG_{22}, $\Delta\lambda_1$, $\Delta\lambda_2$, $\Delta\epsilon$, and $\Delta\Sigma$ have been standardized by dividing by their means, whereas ΔG_{12} and $\Delta\varphi$ are raw values. Due to space constraints, we present only means here. In most cases, the standard deviations are much smaller than the means. However, for the angle measure, φ, the standard deviation is much larger than the mean, except when r_ω is large. Under these parameter values, the SHC approximation (see text) for the expected genetic variances of a single trait are 0.51 and 0.25 for ω values of 49 and 9, respectively.

ω_{11}	ω_{22}	r_ω	G_{11}	G_{22}	G_{12}	r_g	λ_1	λ_2	Σ	ϵ	φ	ΔG_{11}	ΔG_{22}	ΔG_{12}	$\Delta\lambda_1$	$\Delta\lambda_2$	$\Delta\Sigma$	$\Delta\epsilon$	$\Delta\varphi$
9	9	0	0.201	0.192	0.008	0.044	0.24	0.15	0.39	0.64	8.7	0.074	0.075	0.010	0.062	0.091	0.055	0.10	9.51
9	9	0.25	0.187	0.180	0.016	0.089	0.23	0.14	0.37	0.63	16.6	0.074	0.075	0.009	0.066	0.087	0.055	0.10	9.34
9	9	0.50	0.176	0.164	0.034	0.201	0.22	0.12	0.34	0.57	31.2	0.074	0.075	0.009	0.071	0.080	0.056	0.10	7.46
9	9	0.75	0.141	0.150	0.047	0.306	0.20	0.09	0.29	0.48	41.7	0.076	0.075	0.008	0.074	0.080	0.058	0.11	5.28
9	9	0.85	0.117	0.123	0.047	0.373	0.17	0.07	0.24	0.43	44.0	0.077	0.076	0.007	0.075	0.081	0.060	0.11	4.30
9	9	0.90	0.113	0.111	0.049	0.416	0.17	0.06	0.22	0.40	43.0	0.077	0.077	0.007	0.076	0.083	0.062	0.11	3.92
49	49	0	0.432	0.443	0.012	0.028	0.54	0.33	0.88	0.63	5.9	0.072	0.072	0.022	0.059	0.091	0.053	0.10	9.10
49	49	0.25	0.419	0.422	0.021	0.042	0.52	0.32	0.84	0.62	8.5	0.072	0.072	0.021	0.061	0.088	0.053	0.10	9.21
49	49	0.50	0.422	0.427	0.053	0.117	0.53	0.32	0.85	0.62	25.6	0.072	0.072	0.022	0.066	0.080	0.053	0.10	8.92
49	49	0.75	0.349	0.368	0.068	0.177	0.46	0.26	0.72	0.60	35.0	0.072	0.072	0.018	0.068	0.077	0.053	0.10	7.83
49	49	0.85	0.307	0.301	0.095	0.304	0.41	0.19	0.61	0.50	41.0	0.076	0.073	0.016	0.071	0.074	0.055	0.10	5.41
49	49	0.90	0.280	0.267	0.101	0.364	0.39	0.16	0.55	0.44	41.5	0.072	0.073	0.015	0.072	0.075	0.056	0.10	4.30
49	9	0	0.356	0.216	−0.006	−0.019	0.38	0.20	0.57	0.55	−3.2	0.073	0.074	0.014	0.054	0.110	0.055	0.10	6.60
49	9	0.25	0.378	0.216	0.018	0.062	0.39	0.20	0.59	0.53	6.1	0.072	0.075	0.015	0.061	0.096	0.055	0.10	6.29
49	9	0.50	0.340	0.206	0.042	0.152	0.37	0.18	0.55	0.51	14.3	0.073	0.075	0.014	0.067	0.085	0.056	0.10	5.68
49	9	0.75	0.280	0.156	0.052	0.235	0.31	0.13	0.44	0.45	19.3	0.073	0.075	0.011	0.070	0.082	0.057	0.10	4.39
49	9	0.85	0.286	0.130	0.068	0.336	0.32	0.10	0.42	0.35	20.3	0.073	0.075	0.010	0.072	0.080	0.059	0.11	3.02
49	9	0.90	0.246	0.110	0.061	0.344	0.27	0.08	0.36	0.34	20.3	0.074	0.077	0.009	0.073	0.082	0.060	0.11	3.02
99	99	0	0.561	0.519	0.004	0.007	0.66	0.42	1.08	0.65	4.2	0.071	0.072	0.027	0.057	0.091	0.052	0.10	9.55
99	49	0	0.504	0.463	0.015	0.038	0.60	0.37	0.97	0.62	8.4	0.072	0.072	0.024	0.058	0.091	0.053	0.10	9.03
99	19	0	0.455	0.354	−0.011	−0.028	0.50	0.30	0.81	0.63	−4.6	0.072	0.072	0.020	0.056	0.097	0.053	0.10	8.79
99	9	0	0.375	0.224	0.011	0.035	0.40	0.20	0.60	0.55	3.7	0.072	0.074	0.015	0.058	0.100	0.055	0.10	6.68
99	4	0	0.351	0.144	0.000	0.006	0.36	0.14	0.50	0.41	0.8	0.073	0.075	0.011	0.050	0.134	0.057	0.10	3.75

TABLE 2. The influence of population size on **G**-matrix stability during stabilizing selection. The following parameters are fixed: $\omega_{11} = \omega_{22} = 49$, $\alpha_1^2 = \alpha_2^2 = 0.05$. See the text and Table 1 for more information about other parameter values, methods, and the meaning of symbols. Note that the parameters used in the first five rows of this table correspond to those used to generate Figures 2–5. For these parameter values, the SHC-expected genetic variances (see text) are 0.51, 0.81, 1.15, and 1.46 for N_es of 342, 683, 1366, and 2731, respectively.

| N_e	r_ω	r_μ	G_{11}	G_{22}	G_{12}	r_g	λ_1	λ_2	ϵ	Σ	φ	ΔG_{11}	ΔG_{22}	ΔG_{12}	$\Delta\lambda_1$	$\Delta\lambda_2$	$\Delta\Sigma$	$\Delta\epsilon$	$\Delta\varphi$
342	0	0	0.432	0.443	0.012	0.028	0.54	0.33	0.63	0.88	5.9	0.072	0.072	0.022	0.059	0.091	0.05	0.10	9.10
342	0.75	0	0.355	0.353	0.062	0.164	0.46	0.25	0.58	0.71	28.6	0.072	0.072	0.018	0.071	0.072	0.05	0.10	7.48
342	0	0.50	0.408	0.399	0.167	0.411	0.59	0.22	0.44	0.81	42.4	0.072	0.072	0.022	0.071	0.072	0.06	0.10	3.64
342	0.75	0.50	0.410	0.399	0.226	0.548	0.64	0.17	0.29	0.81	44.7	0.072	0.072	0.024	0.072	0.072	0.06	0.10	2.34
342	0.90	0.90	0.465	0.467	0.419	0.895	0.89	0.05	0.05	0.93	45.0	0.071	0.072	0.032	0.072	0.071	0.07	0.10	0.71
683	0	0	0.658	0.660	0.013	0.022	0.77	0.55	0.71	1.32	2.8	0.051	0.051	0.023	0.044	0.059	0.04	0.07	8.80
683	0.75	0	0.477	0.470	0.127	0.260	0.62	0.33	0.56	0.95	42.1	0.051	0.051	0.018	0.050	0.051	0.04	0.07	4.24
683	0	0.50	0.598	0.599	0.228	0.381	0.84	0.36	0.44	1.20	45.0	0.051	0.051	0.023	0.051	0.051	0.04	0.07	2.65
683	0.75	0.50	0.628	0.603	0.350	0.563	0.97	0.26	0.28	1.23	43.8	0.051	0.051	0.025	0.051	0.051	0.04	0.07	1.51
683	0.90	0.90	0.663	0.639	0.580	0.890	1.23	0.07	0.06	1.30	44.4	0.051	0.051	0.031	0.051	0.050	0.05	0.07	0.52
1366	0	0	0.853	0.840	-0.004	-0.003	0.95	0.75	0.79	1.69	0.6	0.036	0.036	0.021	0.031	0.040	0.03	0.05	9.71
1366	0.75	0	0.591	0.587	0.211	0.352	0.81	0.37	0.47	1.18	45.1	0.036	0.036	0.016	0.036	0.036	0.03	0.05	2.02
1366	0	0.50	0.796	0.790	0.292	0.366	1.10	0.49	0.46	1.59	44.4	0.036	0.036	0.021	0.036	0.036	0.03	0.05	1.88
1366	0.75	0.50	0.746	0.740	0.447	0.597	1.19	0.29	0.25	1.49	44.8	0.036	0.036	0.022	0.036	0.036	0.03	0.05	0.99
1366	0.90	0.90	0.806	0.813	0.722	0.891	1.53	0.09	0.06	1.62	45.2	0.036	0.036	0.028	0.036	0.036	0.03	0.05	0.37
2731	0	0	0.937	0.911	-0.007	-0.007	1.02	0.83	0.82	1.85	-3.5	0.025	0.025	0.016	0.023	0.028	0.02	0.03	7.60
2731	0.75	0	0.650	0.676	0.271	0.406	0.94	0.39	0.42	1.33	46.5	0.025	0.025	0.013	0.025	0.026	0.02	0.04	1.16
2731	0	0.50	0.914	0.896	0.269	0.298	1.18	0.63	0.54	1.81	44.1	0.025	0.025	0.017	0.025	0.025	0.02	0.04	1.68
2731	0.75	0.50	0.820	0.832	0.520	0.629	1.35	0.30	0.23	1.65	45.3	0.025	0.025	0.017	0.025	0.025	0.02	0.04	0.63
2731	0.90	0.90	0.950	0.931	0.840	0.893	1.78	0.10	0.06	1.88	44.7	0.025	0.025	0.022	0.025	0.025	0.02	0.04	0.26
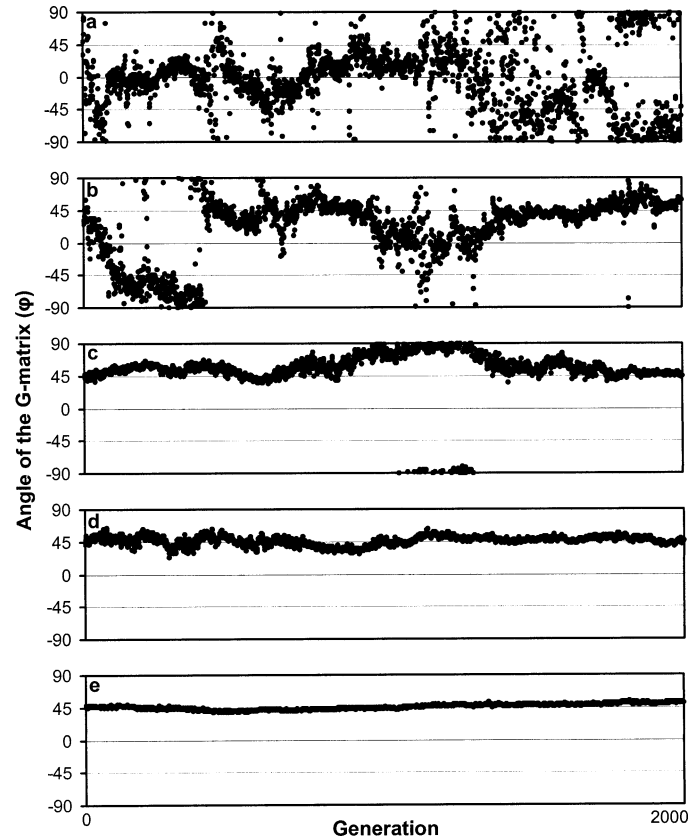
FIG. 2. Time series of the orientation, φ, the angle between the leading eigenvector and the x-axis. Each figure displays the angle φ from one replicate run near stochastic equilibrium for 2000 generations. As in Figure 3, from top to bottom, the following selectional and mutational correlations are chosen: (**a**) $r_\mu = r_\omega = 0$; (**b**) $r_\mu = 0$, $r_\omega = 0.75$; (**c**) $r_\mu = 0.5$, $r_\omega = 0$; (**d**) $r_\mu = 0.5$, $r_\omega = 0.75$; (**e**) $r_\mu = r_\omega = 0.90$. This figure was produced using the same parameter values as those used for Figure 3.

strength). However, it has larger effects on the average eigenvalues. Increasing the mutational correlation r_μ always increases the leading eigenvalue but decreases the minor one. Accordingly, the eccentricity increases substantially, that is, the shape parameter ϵ gets very small and the genetic covariance and correlation increase strongly. In other words, mutational correlation strongly promotes a cigar-shaped **G**-matrix.

As in Table 1, the between-generation changes of the genetic variances, hence of the overall size, as well as of the shape, are virtually unaffected by varying the mutational correlation. However, because $\Delta\epsilon$ (as well as ΔG_{11} and ΔG_{22}) is measured relative to the mean and the mean ϵ is very small for large r_μ, the absolute change in shape is very small if mutational correlation is large. The between-generation change of the eigenvalues is affected in a very similar way by increasing r_μ as by increasing r_ω (cf. with Table 1). However, an increasing mutational correlation leads to much higher stability of the orientation, that is, small $\Delta\varphi$. The average per-generation change in the genetic covariance (ΔG_{12}) increases slightly as r_μ increases. However, this increase is associated with a dramatic increase in the average magnitude of the genetic covariance. Thus, relative to its mean, ΔG_{12}

TABLE 3. The influence of mutational correlation on **G**-matrix stability during stabilizing selection. The following parameters are fixed: $N_e = 342$, $r_\omega = 0$, $\alpha_1^2 = \alpha_2^2 = 0.05$. See text and Table 1 for additional information regarding other parameter values, methods, symbol definitions, and expected levels of genetic variance according to the SHC approximation.

ω_{11}	ω_{22}	r_μ	G_{11}	G_{22}	G_{12}	r_g	λ_1	λ_2	Σ	ϵ	φ	ΔG_{11}	ΔG_{22}	ΔG_{12}	$\Delta\lambda_1$	$\Delta\lambda_2$	$\Delta\Sigma$	$\Delta\epsilon$	$\Delta\varphi$
9	9	0	0.188	0.195	0.003	0.012	0.24	0.15	0.38	0.65	2.0	0.075	0.075	0.010	0.060	0.096	0.06	0.10	9.35
9	9	0.25	0.192	0.197	0.031	0.161	0.25	0.14	0.39	0.59	27.5	0.074	0.075	0.010	0.068	0.082	0.06	0.10	7.92
9	9	0.50	0.183	0.178	0.067	0.361	0.26	0.11	0.36	0.40	42.9	0.075	0.075	0.010	0.075	0.075	0.06	0.10	4.37
9	9	0.75	0.178	0.167	0.097	0.556	0.27	0.07	0.34	0.18	43.0	0.074	0.075	0.010	0.075	0.073	0.06	0.10	2.30
9	9	0.85	0.166	0.168	0.117	0.693	0.29	0.05	0.33	0.12	45.5	0.075	0.075	0.011	0.075	0.073	0.07	0.10	1.55
9	9	0.90	0.162	0.165	0.129	0.700	0.29	0.03	0.33	0.08	45.4	0.075	0.075	0.011	0.075	0.072	0.07	0.10	1.16
49	49	0	0.439	0.453	-0.019	-0.045	0.55	0.35	0.89	0.63	-10.0	0.072	0.072	0.023	0.055	0.096	0.05	0.10	9.90
49	49	0.25	0.452	0.444	0.068	0.156	0.57	0.33	0.90	0.59	25.2	0.072	0.072	0.023	0.066	0.079	0.05	0.10	7.88
49	49	0.50	0.408	0.399	0.167	0.411	0.59	0.22	0.81	0.44	42.4	0.072	0.072	0.022	0.071	0.072	0.06	0.10	3.64
49	49	0.75	0.412	0.408	0.282	0.686	0.70	0.12	0.82	0.28	44.7	0.072	0.072	0.025	0.072	0.071	0.06	0.10	1.54
49	49	0.85	0.405	0.418	0.327	0.790	0.74	0.08	0.82	0.18	45.7	0.073	0.073	0.027	0.073	0.071	0.07	0.10	1.12
49	49	0.90	0.409	0.405	0.348	0.848	0.76	0.06	0.81	0.12	44.8	0.073	0.073	0.028	0.073	0.070	0.07	0.10	0.90
49	9	0	0.342	0.227	0.012	0.043	0.37	0.20	0.57	0.58	5.1	0.072	0.074	0.014	0.059	0.096	0.05	0.10	7.13
49	9	0.25	0.365	0.236	0.042	0.162	0.40	0.20	0.60	0.51	18.1	0.073	0.073	0.015	0.065	0.087	0.05	0.10	5.77
49	9	0.50	0.331	0.224	0.114	0.413	0.41	0.14	0.56	0.37	32.8	0.073	0.073	0.015	0.073	0.073	0.06	0.10	3.18
49	9	0.75	0.282	0.224	0.153	0.608	0.41	0.09	0.51	0.24	39.9	0.073	0.074	0.015	0.074	0.073	0.06	0.10	1.92
49	9	0.85	0.275	0.224	0.181	0.727	0.43	0.06	0.50	0.16	40.9	0.073	0.074	0.016	0.074	0.072	0.07	0.10	1.37
49	9	0.90	0.258	0.227	0.197	0.809	0.44	0.04	0.48	0.10	42.6	0.073	0.073	0.016	0.074	0.072	0.07	0.10	1.05

becomes very small as r_μ increases. Asymmetric selection strength increases stability of the orientation slightly if the mutational correlation is low, but not otherwise. Thus, mutational correlation may be an important agent in stabilizing the orientation of a **G**-matrix; it does not, however, stabilize its size or shape.

To investigate more fully the role of the pattern of pleiotropic mutations in determining the shape and orientation of the **G**-matrix, we also performed simulations in which the mutational variances of the traits differed, but without any selectional or mutational correlation. The results presented in Table 4 clearly demonstrate that for symmetric selection on the two traits, increasingly different mutational variances increase the eccentricity of the **G**-matrix and enhance stability of the orientation. Clearly, the total size Σ of the **G**-matrix is strongly correlated with the total mutational variance. Unequal mutational variances do not at all affect the stability in size or shape. The same is true for asymmetric stabilizing selection. However, instability of the orientation is maximized under asymmetric stabilizing selection if the mutational variance of the trait under weaker selection is somewhat, but not much, higher than that of the other trait.

The Effect of Population Size on **G**-matrix Stability

Almost all the variation in the size of the **G**-matrix, as measured by the genetic variances and the total variance, is due to random genetic drift. This is clearly demonstrated by Table 2. Also, the between-generation change of the eigenvalues and all other measures of instability decrease with increasing population size. Increasing population size has a slight increasing effect on the shape parameter ϵ unless mutational and selectional correlation both are strong, but almost no effect on the orientation φ. The between-generation change $\Delta\epsilon$ decreases with increasing population size. Increasing population size has only a weak effect on the stability in orientation, $\Delta\varphi$, and increases stability most if correlational selection is strong or if there is substantial mutational correlation.

Mutation Rate Considerations

The per-locus mutation rate that we employed for the majority of our analyses may be unrealistically high for single loci affecting quantitative traits (Kondrashov 2003). Justification for our use of this high mutation rate comes from two sources. First, if several physically linked loci affect the same trait, then they can behave as a single locus with a higher mutation rate (Bürger 2000). If this phenomenon is common, it would justify the use of a mutation rate considerably higher than the empirically estimated single-locus mutation rate. Second, this mutation rate is necessary to maintain genetic variation in the small populations under consideration in this study, given the assumption that each trait is determined by 50 loci. Small population size was a necessary constraint in this study, because the Monte Carlo simulations become very slow as population size increases.

To test the validity of our conclusions for loci with smaller mutation rates, we performed some simulations with mutation rates of 1×10^{-4} and 2×10^{-5} per locus per generation. The results of these simulations are presented in Table 5.

TABLE 4. The influence of mutational variance on **G**-matrix stability during stabilizing selection. The following parameters are fixed: $N_e = 342$, $r_\omega = r_\mu = 0$, $\alpha_1^2 = 0.05$. See the text and Table 1 for more information about other parameter values, methods, and the meaning of symbols. In no case does the angle measure, φ, differ significantly from zero, which is to be expected because without mutational or selectional correlation no mechanism is present to produce a nonzero angle. Note that the fourth column shows the expected genetic variance for the second trait according to the SHC approximation (see text).

ω_{11}	ω_{22}	α_2^2	$\hat{G}_{22}$	G_{11}	G_{22}	G_{12}	r_g	λ_1	λ_2	Σ	ϵ	φ	ΔG_{11}	ΔG_{22}	ΔG_{12}	$\Delta\lambda_1$	$\Delta\lambda_2$	$\Delta\Sigma$	$\Delta\epsilon$	$\Delta\varphi$
9	9	0.01	0.10	0.223	0.072	0.000	−0.005	0.23	0.07	0.30	0.32	−0.1	0.073	0.073	0.006	0.046	0.161	0.06	0.10	2.59
9	9	0.02	0.16	0.213	0.112	0.001	0.008	0.22	0.01	0.33	0.49	1.3	0.074	0.073	0.008	0.054	0.116	0.06	0.10	5.39
9	9	0.03	0.20	0.211	0.146	0.000	0.006	0.23	0.13	0.36	0.59	0.4	0.074	0.073	0.009	0.057	0.102	0.06	0.10	7.84
9	9	0.05	0.25	0.188	0.195	0.003	0.012	0.24	0.15	0.38	0.65	2.0	0.075	0.075	0.010	0.060	0.096	0.06	0.10	9.35
9	9	0.10	0.31	0.164	0.237	0.004	0.022	0.26	0.14	0.40	0.57	5.9	0.075	0.077	0.010	0.061	0.102	0.06	0.10	7.66
9	9	0.20	0.35	0.139	0.286	−0.003	−0.019	0.30	0.13	0.43	0.45	−7.0	0.077	0.081	0.011	0.055	0.137	0.06	0.10	4.83
49	49	0.01	0.13	0.484	0.120	0.002	0.003	0.49	0.11	0.60	0.25	−0.0	0.072	0.071	0.012	0.045	0.184	0.06	0.10	1.93
49	49	0.02	0.24	0.479	0.207	−0.003	−0.020	0.49	0.10	0.69	0.41	−1.8	0.072	0.072	0.016	0.049	0.129	0.06	0.10	3.75
49	49	0.03	0.34	0.427	0.279	−0.002	−0.002	0.46	0.25	0.71	0.57	1.4	0.072	0.073	0.017	0.054	0.102	0.05	0.10	7.16
49	49	0.05	0.51	0.439	0.453	−0.019	−0.045	0.55	0.35	0.89	0.63	−10.0	0.072	0.072	0.023	0.055	0.096	0.05	0.10	9.90
49	49	0.10	0.81	0.428	0.698	0.013	0.025	0.74	0.39	1.13	0.54	5.0	0.072	0.073	0.028	0.055	0.103	0.05	0.10	6.59
49	49	0.20	1.16	0.370	0.995	0.006	0.007	1.01	0.35	1.36	0.36	4.2	0.073	0.074	0.031	0.051	0.139	0.06	0.10	3.11
49	9	0.01	0.10	0.449	0.093	0.003	0.012	0.45	0.09	0.54	0.21	0.2	0.072	0.072	0.010	0.046	0.202	0.06	0.10	1.72
49	9	0.02	0.16	0.440	0.143	−0.007	−0.033	0.45	0.14	0.58	0.33	−1.9	0.072	0.073	0.013	0.044	0.165	0.06	0.10	2.66
49	9	0.03	0.20	0.395	0.183	−0.002	−0.004	0.41	0.17	0.58	0.45	−0.2	0.072	0.073	0.014	0.052	0.121	0.06	0.10	4.21
49	9	0.05	0.25	0.342	0.227	0.012	0.043	0.37	0.20	0.57	0.58	5.1	0.072	0.074	0.014	0.059	0.096	0.05	0.10	7.13
49	9	0.10	0.31	0.313	0.286	0.006	0.019	0.37	0.23	0.60	0.63	4.5	0.073	0.076	0.015	0.061	0.092	0.05	0.10	9.47
49	9	0.20	0.35	0.255	0.356	−0.008	−0.027	0.39	0.21	0.61	0.57	−6.4	0.074	0.078	0.016	0.057	0.109	0.06	0.10	7.59
9	49	0.01	0.13	0.245	0.087	0.001	0.005	0.25	0.08	0.33	0.36	−0.1	0.073	0.072	0.007	0.049	0.142	0.06	0.10	2.97
9	49	0.02	0.24	0.231	0.165	0.003	0.009	0.25	0.14	0.40	0.58	1.3	0.073	0.072	0.010	0.057	0.097	0.05	0.10	7.58
9	49	0.03	0.34	0.244	0.240	−0.009	−0.031	0.30	0.19	0.48	0.65	−8.6	0.074	0.072	0.012	0.056	0.096	0.05	0.10	9.79
9	49	0.05	0.51	0.227	0.342	0.012	0.043	0.37	0.20	0.57	0.58	5.1	0.074	0.072	0.014	0.059	0.096	0.05	0.10	7.13
9	49	0.10	0.81	0.214	0.586	−0.006	−0.017	0.60	0.20	0.80	0.36	−8.2	0.074	0.073	0.018	0.046	0.154	0.06	0.10	3.16
9	49	0.20	1.16	0.202	0.818	−0.017	−0.034	0.83	0.19	1.02	0.24	−10.5	0.074	0.075	0.021	0.042	0.215	0.06	0.10	2.01

TABLE 5. The influence of the mutation rate (μ) on **G**-matrix stability. The following parameters are fixed: $\omega_{11} = \omega_{22} = 49$, $\alpha_1^2 = \alpha_2^2 = 0.05$, $N_e = 1366$. See the text and Table 1 for more information about other parameter values, methods, and the meaning of symbols. Note that the first five rows repeat results from Table 4 for comparison.

μ	r_ω	r_μ	G_{11}	G_{22}	G_{12}	r_g	λ_1	λ_2	Σ	ϵ	φ	ΔG_{11}	ΔG_{22}	ΔG_{12}	$\Delta\lambda_1$	$\Delta\lambda_2$	$\Delta\Sigma$	$\Delta\epsilon$	$\Delta\varphi$
2×10^{-4}	0	0	0.853	0.840	−0.004	−0.003	0.95	0.75	1.69	0.79	0.6	0.036	0.036	0.021	0.031	0.040	0.03	0.05	9.71
2×10^{-4}	0.75	0	0.591	0.587	0.211	0.352	0.81	0.37	1.18	0.47	45.1	0.036	0.036	0.016	0.036	0.036	0.03	0.05	2.02
2×10^{-4}	0	0.50	0.796	0.790	0.292	0.366	1.10	0.49	1.59	0.46	44.4	0.036	0.036	0.021	0.036	0.036	0.03	0.05	1.88
2×10^{-4}	0.75	0.50	0.746	0.740	0.447	0.597	1.19	0.29	1.49	0.25	44.8	0.036	0.036	0.022	0.036	0.036	0.03	0.05	0.99
2×10^{-4}	0.90	0.90	0.806	0.813	0.722	0.891	1.53	0.09	1.62	0.06	45.2	0.036	0.036	0.028	0.036	0.036	0.03	0.05	0.37
1×10^{-4}	0	0	0.438	0.409	0.006	0.014	0.48	0.36	0.85	0.76	3.3	0.036	0.036	0.011	0.035	0.036	0.03	0.05	8.18
1×10^{-4}	0.75	0	0.285	0.302	0.097	0.327	0.40	0.19	0.59	0.49	46.9	0.037	0.036	0.008	0.036	0.037	0.03	0.05	2.19
1×10^{-4}	0	0.50	0.408	0.398	0.138	0.337	0.55	0.26	0.81	0.49	43.0	0.036	0.036	0.011	0.036	0.036	0.03	0.05	2.48
1×10^{-4}	0.75	0.50	0.401	0.399	0.246	0.613	0.65	0.15	0.80	0.24	44.9	0.036	0.036	0.012	0.036	0.037	0.03	0.05	0.94
1×10^{-4}	0.90	0.90	0.443	0.457	0.404	0.898	0.86	0.04	0.90	0.05	45.5	0.036	0.036	0.015	0.036	0.036	0.03	0.05	0.35
2×10^{-5}	0	0	0.077	0.081	−0.001	0.023	0.11	0.05	0.16	0.50	−1.4	0.040	0.039	0.002	0.039	0.042	0.03	0.06	3.54
2×10^{-5}	0.75	0	0.050	0.060	0.019	0.344	0.08	0.03	0.11	0.38	40.7	0.042	0.040	0.002	0.040	0.046	0.03	0.06	2.09
2×10^{-5}	0	0.50	0.089	0.086	0.032	0.371	0.13	0.05	0.17	0.39	37.3	0.039	0.039	0.002	0.038	0.039	0.03	0.05	2.06
2×10^{-5}	0.75	0.50	0.065	0.067	0.040	0.595	0.11	0.02	0.13	0.25	45.4	0.041	0.040	0.002	0.040	0.042	0.03	0.06	1.25
2×10^{-5}	0.90	0.90	0.093	0.096	0.084	0.876	0.18	0.01	0.19	0.07	45.9	0.039	0.039	0.003	0.039	0.039	0.04	0.05	0.42

The smaller mutation rates produce results that are very similar to the results with higher mutation rates. The major difference is that the amount of standing genetic variance is substantially reduced, resulting in a decrease in Σ. Even though these low mutation rates eliminate most of the genetic variance in the population, resulting in trait heritabilities less than 0.10 in the most extreme case, the patterns of change in the **G**-matrix remain remarkably similar to the simulations with much greater genetic variance. Thus, our main conclusions appear to be robust to large changes in the per locus mutation rate.

The Influence of Alignment on G-matrix Evolution

Another issue concerns the interplay of selectional and mutational correlations. It is to be expected that alignment between the selection matrix, determining the shape of the adaptive surface, and the matrix of mutational effects enhances stability. This is indeed borne out by our numerical results. Figure 1 displays the change in orientation of the **G**-matrix as a function of the selectional correlation r_ω for five different values of r_μ. This figure clearly shows that for positive mutational correlation, the between-generation change of the angle, $\Delta\varphi$, always decreases with increasing selectional correlation unless the mutational correlation is very weak. Put otherwise, mutational and selectional correlations of different signs lead to instability of the orientation. Without mutational correlation, any increase in selection correlation, positive or negative, clearly increases stability of the orientation. Figure 1 also demonstrates that mutational correlation is much more important in producing stability than correlational selection.

Visualizing the Evolution of the G-matrix

Figure 3 depicts the change of the size, shape, and orientation of the **G**-matrix within one replicate run under each of five different scenarios by displaying snapshots of graphical representations of the **G**-matrix at intervals of 200 generations. Whereas the **G**-matrix apparently is fluctuating and flipping around randomly if $r_\mu = r_\omega = 0$, with no visible difference in the case of $r_\omega = 0.75$, fluctuations of the shape and orientation (but not size) are markedly restricted in the two cases where $r_\mu = 0.5$. Obviously, increasing selectional correlation substantially aids their stability. The case of $r_\mu = r_\omega = 0.90$ results in a highly stable **G**-matrix that is extremely cigar-shaped. It still fluctuates in size, however.

Figure 2 displays the complete time series of the angle φ between the leading eigenvector and the *x*-axis for the five runs shown in Figure 3. Because the angle is confined to the interval $-90°$ to $+90°$, and, for example, 95° corresponds to $-85°$, flipping from near $-90°$ to near $+90°$ does not imply a great change in the **G**-matrix. It is interesting to observe the high degree of autocorrelation for the runs without mutational or selectional correlation. Often, the orientation stays around the same value for hundreds of generations before changing substantially. Figure 2b also shows distinctively that with strong selectional correlation but not mutational correlation, there are prolonged periods during which the orientation remains quite stable (e.g., between about generations 1500 to 1700), whereas during other periods (between
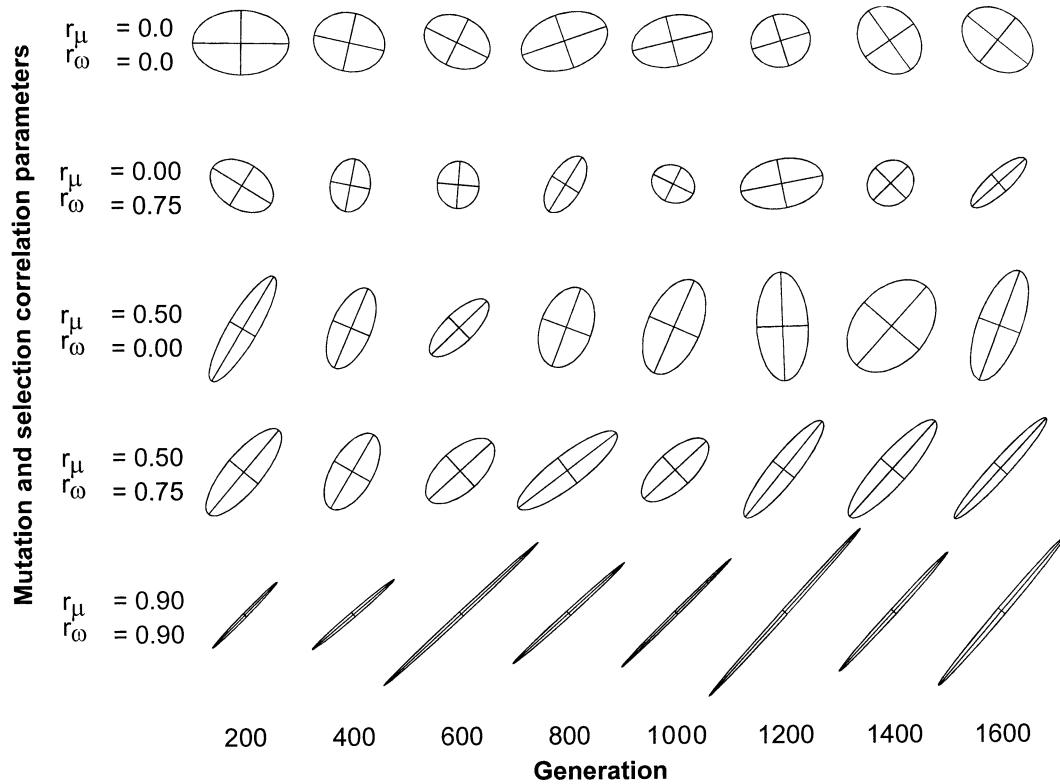
FIG. 3. Time dependence of size, shape, and orientation of the **G**-matrix, displayed as ellipses with axis length proportional to the corresponding eigenvalues. These are snapshots, taken every 200th generation, each from a single replicate run. From top to bottom, the following selectional and mutational correlations are chosen: (**a**) $r_\mu = r_\omega = 0$; (**b**) $r_\mu = 0$, $r_\omega = 0.75$; (**c**) $r_\mu = 0.5$, $r_\omega = 0$; (**d**) $r_\mu = 0.5$, $r_\omega = 0.75$; (**e**) $r_\mu = r_\omega = 0.90$. The following parameters are the same for all panels: $N_e = 342$, $\omega_{11} = \omega_{22} = 49$, $\alpha_1^2 = \alpha_2^2 = 0.05$.

generations 1000 and 1300) the orientation is flipping around wildly. Figures 2d and 2e demonstrate to what extent moderate to high selectional and mutational correlations can stabilize the orientation of the **G**-matrix provided they are of the same sign and of similar magnitude. Despite this amazing stability in orientation, there is still substantial variation in the size (Σ) of these **G**-matrices (Fig. 4). Figure 5 shows the time series for the eccentricity (ϵ) of the **G**-matrix from the same runs as those shown in Figures 2, 3, and 4. Even though the change in eccentricity, when standardized to the mean, does not change as a consequence of mutational or selectional correlation, the magnitude of ϵ becomes so small as correlations stabilize the angle φ that the **G**-matrix retains its overall shape for extremely long spans of time.

The Reduction of Genetic Variance Due to Pleiotropy

Stabilizing selection on multiple traits determined by pleiotropic loci is expected to reduce the genetic variance of these traits relative to what would be expected if each trait were determined by a completely independent set of loci. Indeed, our simulations verify that pleiotropy does decrease the equilibrium level of additive genetic variance, as predicted by models developed by Turelli (1985) and Wagner (1989). This reduction of variance due to pleiotropy is obvious when we consider the SHC-approximation for the expected genetic variance of a single trait. In all cases that we investigated (see Tables 1–5), the expected genetic variance according to the SHC model was higher than the amount of

genetic variance that we observed in our simulated populations.

DISCUSSION

Our simulations show that the **G**-matrix is stable under some conditions and unstable under others. This result helps define a central issue in evolutionary genetics. Following on the heels of Lande's (1979, 1980) pioneering papers, this central issue was cast in terms of **G**-matrix constancy. Lande's models assumed **G**-matrix constancy. Is that proposition literally true? Because the proposition of literal constancy is easily refuted from first principles (Turelli 1988; Shaw et al. 1995) and, sometimes, on empirical grounds (Arnold and Phillips 1999), some workers have considered the issue settled. Clearly the **G**-matrix is not constant. This characterization, however, trivializes the constancy issue and so achieves closure prematurely. The primary claim of this article is that the constancy issue has deeper ramifications and can be approached by asking three questions. First, under what conditions is the **G**-matrix stable and under what conditions is it unstable? Second, how common are conditions promoting stability or instability in nature? And third, how much and what kind of stability is required to make meaningful extrapolations of equations for drift or response to selection? This article focuses on the first question. Previous studies correctly identified several factors that contribute to stability but were unable to assess their relative importance (Turelli 1988). We found that stable orientation of the **G**-
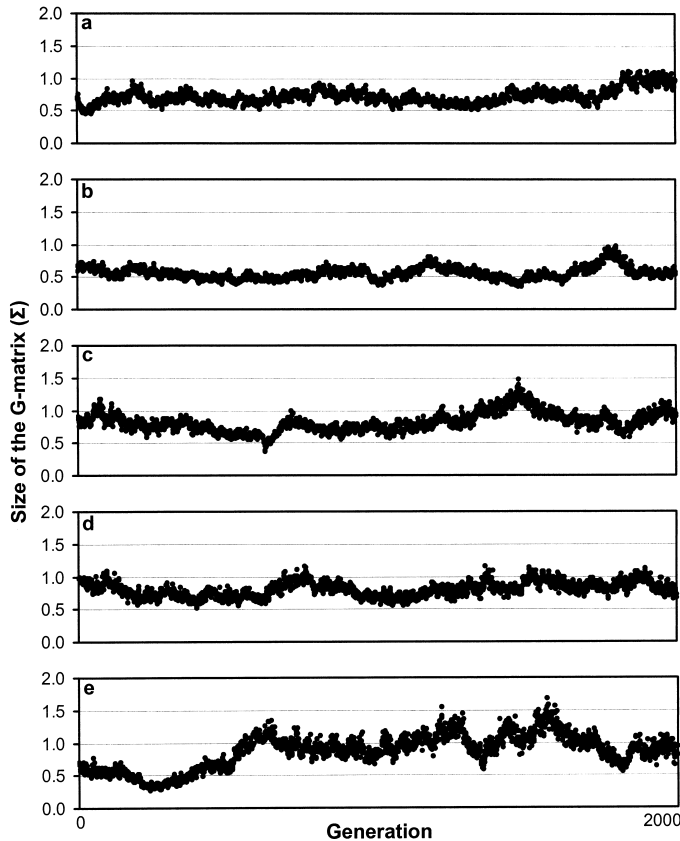
FIG. 4. Time series of the size of the **G**-matrix, Σ, the sum of the genetic variances, which is equal to the sum of the eigenvalues. As in Figure 3, from top to bottom, the following selectional and mutational correlations are chosen: (**a**) $r_\mu = r_\omega = 0$; (**b**) $r_\mu = 0$, $r_\omega = 0.75$; (**c**) $r_\mu = 0.5$, $r_\omega = 0$; (**d**) $r_\mu = 0.5$, $r_\omega = 0.75$; (**e**) $r_\mu = r_\omega = 0.90$. This figure was produced using the same parameter values as those used for Figure 3.

FIG. 5. Time series of the eccentricity of the **G**-matrix, ϵ, the smaller eigenvalue divided by the larger eigenvalue. As in Figure 3, from top to bottom, the following selectional and mutational correlations are chosen: (**a**) $r_\mu = r_\omega = 0$; (**b**) $r_\mu = 0$, $r_\omega = 0.75$; (**c**) $r_\mu = 0.5$, $r_\omega = 0$; (**d**) $r_\mu = 0.5$, $r_\omega = 0.75$; (**e**) $r_\mu = r_\omega = 0.90$. This figure was produced using the same parameter values as those used for Figure 3.

matrix is promoted by correlational selection, large population size, and especially by pleiotropic mutation. The highest levels of instability prevailed in small populations with no correlational selection and no mutational correlation.

The recognition of different kinds of **G**-matrix stability is an important contribution of the present study. By characterizing the **G**-matrix in terms of its eigenvalues and eigenvectors, we can recognize three varieties of stability that are related to the size, shape, and orientation of the matrix. The importance of recognizing these three kinds of stability is emphasized by our finding that they respond differently to various conditions. Thus, size and shape stability are promoted chiefly by large population size. In contrast, orientation stability is promoted by pleiotropic mutation, correlational selection, and the alignment of these two processes (in addition to large population size). This result of differential sensitivity to conditions supports the view that comparative studies of the **G**-matrix should focus on both eigenvalues and eigenvectors (Phillips and Arnold 1999). This type of focus is necessary, because a complete description of the **G**-matrix requires knowledge of the eigenvectors as well as the eigenvalues. In addition, this approach is appealing because ei-
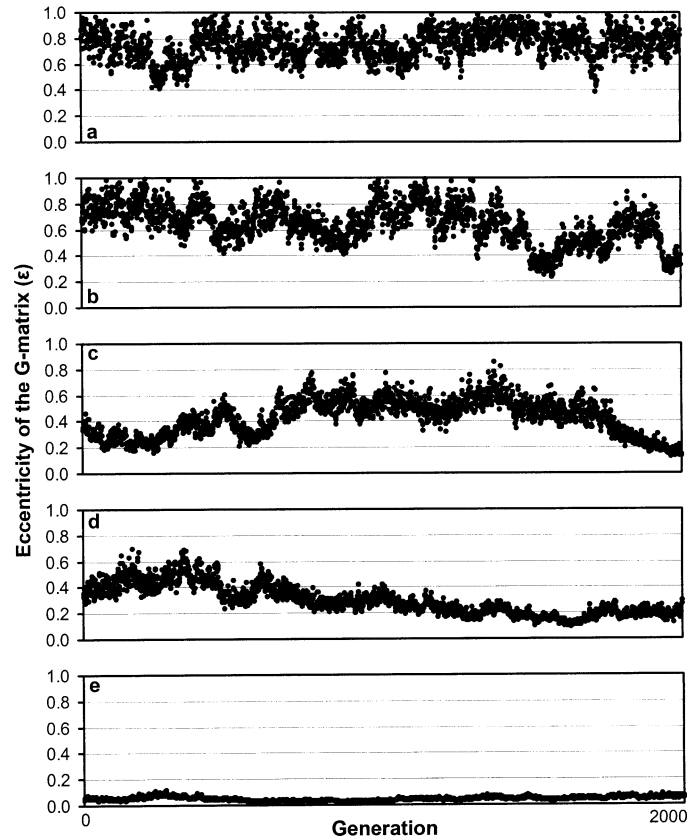
genvalues and eigenvectors provide an intuitive description of the **G**-matrix that lends itself to graphical depiction.

Turning to our second question—the prevalence of stability-promoting conditions in nature—it seems likely that some kinds of characters are more likely than others to have stable **G**-matrices. Thus, bilaterally symmetrical characters may have highly stable **G**-matrices because of strong correlations between mutational effects, as well as strong correlational selection between right and left sides. At the opposite extreme, we may expect fitness components to have unstable **G**-matrices because their adaptive landscapes lack curvature as a consequence of strong, persistent directional selection. Hence, the **G**-matrix for these types of traits will not experience the restraining effects of stabilizing selection. In addition, fitness components are probably determined by a very large number of loci, only some of which may be expected to pleiotropically affect multiple fitness components. Most characters probably lie between these extremes of stability and instability. Although our results provide some expectations about stability, the characterization of **G**-matrix variability for different kinds of characters is fundamentally an empirical exercise.

Our third question—how much stability is necessary for

meaningful extrapolation—is only tangentially addressed by the results presented here. In cases of extreme stability (e.g., Fig. 3e), there can be little doubt that response to selection equations could be accurately extrapolated over many generations. At the opposite extreme, when the **G**-matrix is prone to erratic fluctuation, extrapolations based on the supposition of constancy are bound to be misleading. The parameter space for much of the natural world may lie between these two extremes. One interesting pattern in our results is that the **G**-matrix tended to be unstable when it was less cigar-shaped, whereas the more cigar-shaped **G**-matrices tended to be very stable. Because the more cigar-shaped **G**-matrices are the ones that constrain the evolutionary trajectory, the observed stability of these **G**-matrices may justify extrapolations over many generations. Similarly, even though the less cigar-shaped **G**-matrices were unstable, they constrain the evolutionary trajectory very little in any case, so their instability is less consequential. However, to definitively address this issue we need not only estimates of **G**-matrix stability, but also analyses of how much instability can be tolerated in extrapolations based on matrix averages. Furthermore, Turelli (1988) has pointed out that calculation of the net selection gradient may be complicated not only by fluctuation in **G** but by covariances induced by those fluctuations. One other important consideration is that the conditions for stability under stabilizing selection alone may differ in important ways from the conditions for stability when directional selection is operating. Simulation-based models may provide an expedient way to evaluate these issues.

Some of the present results were anticipated by simulation studies of between-generation change in the genetic variance of a single trait. High autocorrelation in the mean and genetic variance were noted in studies of stabilizing and directional selection on a single trait (Keightley and Hill 1989; Bürger et al. 1989; Bürger and Lande 1994). Strong autocorrelation is a conspicuous feature of **G**-matrix dynamics. In simulations, a particular orientation of the **G**-matrix can be relatively stable for hundreds of generations, but can then change to a new stable orientation or enter a period of chaotic fluctuation. The complex time series for **G**-matrix orientation illustrated in Figure 2 underscores the difficulty of achieving analytical results.

The present results extend our understanding of **G**-matrix evolution based on past studies by computer simulation. Reeve's (2000) main focus was the long-term accuracy of Lande's (1979) equation for the evolution of the multivariate mean. He addressed the issues of **G** evolution and stability only in passing. Although Reeve (2000) explored three different models for the distribution of allelic effects (Gaussian, leptokurtic and biallelic), he did not allow correlational selection and did not report effects on genetic covariance. Hence, Reeve's (2000) analysis did not explicitly address **G**-matrix stability at all, except to note that small changes in the **G**-matrix had little effect on the accuracy of predictions of the response to selection in simulated populations.

Our simulations do not explore some potentially important contributions to **G**-matrix stability or instability. Most notably, we have not addressed the possible effects on **G**-matrix stability of dominance, epistasis, linkage, number of loci, and distributions of allelic effects (including genes of major effect). Likewise, we have only explored cases in which the position and shape of the adaptive landscape and the pattern of mutation are stable. It is likely that some aspects of the dynamics of the **G**-matrix would change if the adaptive landscape were changing, either with respect to the location of its optima, its orientation, or its curvature. These issues are beyond the scope of this initial study, and additional simulation studies are needed to address them.

Our results help to inform the comparative study of **G**-matrices. Under some conditions the **G**-matrix is capable of pronounced, random fluctuation. Under those circumstances, multiple independent samples are needed to make a convincing case for **G**-matrix stability. Thus, neutral or weakly selected characters with little or no genetic correlation in small populations will be especially prone to **G**-matrix fluctuation. Such characters may be poor choices for comparative work, because even considerable effort could yield inconclusive results. In contrast, characters under strong stabilizing and correlational selection with pronounced genetic correlations in large populations are a priori likely to have stable **G**-matrices. Under these conditions, a modest number of samples would be required to make a convincing case for matrix identity or proportionality. Comparative studies should examine multiple aspects of stability because different aspects may be differentially stable. Thus, eigenvalues (size and eccentricity) can show different stability profiles than eigenvectors (orientation). Finally, systematic sampling of matrices on a phylogeny may provide especially revealing data on stability. Under conditions for which the **G**-matrix is likely to be stable, such phylogenetically planned sampling could reveal a pattern of long-term stability in the matrix. This approach may also be the most practical way to obtain convincing evidence for long-term stability in the patterns of stabilizing selection and mutation.

Several unresolved empirical issues are highlighted by our results. Most notably, we need estimates of pleiotropic mutational covariance. Although estimates of mutational variance are available for a number of characters (Lynch 1988; Lynch and Walsh 1998), mutational covariances have seldom been estimated (Camara and Pigliucci 1999). Consequently, we have some basis for choosing parameters for the main diagonal of the mutational matrix but virtually no empirical basis for specification of the off-diagonal elements. Our understanding of multivariate selection is plagued by a similar limitation. Estimates of stabilizing selection are seldom corrected for character correlation (Lande and Arnold 1983; Endler 1986; Kingsolver et al. 2001), and corrected estimates of correlational selection are even less common. Given these limitations, it is not surprising that key issues of alignment are an open field of investigation. Are the matrices describing selection and mutation commonly aligned? Our simulations indicate that such alignment would enhance **G**-matrix stability. Finally, is the adaptive landscape stable on a geological time scale, producing alignment of mutation and inheritance with selection? These are the overarching empirical issues

that will determine how widely quantitative genetic theory can be applied to the natural world.

LITERATURE CITED

Arnold, S. J., and P. C. Phillips. 1999. Hierarchical comparison of genetic variance-covariance matrices. II. Coastal-inland divergence in the garter snake, *Thamnophis elegans*. Evolution 53: 1516–1527.

Arnold, S. J., M. E. Pfrender, and A. G. Jones. 2001. The adaptive landscape as a conceptual bridge between micro- and macro-evolution. Genetica 112–113:9–32.

Baatz, M., and G. P. Wagner. 1997. Adaptive inertia caused by hidden pleiotropic effects. Theor. Popul. Biol. 51:49–66.

Barton, N. H. 1989. Divergence of a polygenic system subject to stabilizing selection, mutation and drift. Genet. Res. 54:59–77.

Begin, M., and D. A. Roff. 2001. An analysis of **G** matrix variation in two closely related cricket species, *Gryllus firmus* and *G. pennsylvanicus*. J. Evol. Biol. 14:1–13.

Billington, H. L., A. M. Mortimer, and T. McNeilly. 1988. Divergence and genetic structure in adjacent grass populations. I. Quantitative genetics. Evolution 42:1267–1277.

Brodie, E. D., III. 1993. Homogeneity of the genetic variance-covariance matrix for antipredator traits in two natural populations of the garter snake *Thamnophis ordinoides*. Evolution 47: 844–854.

Bulmer, M. G. 1972. The genetic variability of polygenic characters under optimizing selection, mutation and drift. Genet. Res. 19: 17–25.

———. 1980. The mathematical theory of quantitative genetics. Clarendon Press, Oxford, U.K.

Bürger, R. 2000. The mathematical theory of selection, recombination, and mutation. John Wiley and Sons, Chichester, U.K.

Bürger, R., and R. Lande. 1994. On the distribution of the mean and variance of a quantitative trait under mutation-selection-drift balance. Genetics 138:901–912.

Bürger, R., and M. Lynch. 1995. Evolution and extinction in a changing environment: a quantitative-genetic analysis. Evolution 49:151–163.

Bürger, R., G. P. Wagner, and F. Stettinger. 1989. How much heritable variation can be maintained in finite populations by mutation-selection balance. Evolution 43:1748–1766.

Camara, M. D., and M. Pigliucci. 1999. Mutational contributions to genetic variance-covariance matrices: an experimental approach using induced mutations in *Arabidopsis thaliana*. Evolution 53:1692–1703.

Crow, J. F., and M. Kimura. 1964. The theory of genetic loads. Pp. 495–505 *in* S. J. Geerts, ed. Proceedings of the XI international congress of genetics. Pergamon, Oxford, U.K.

Endler, J. A. 1986. Natural selection in the wild. Princeton Univ. Press, Princeton, NJ.

Foley, P. 1992. Small population genetic variability at loci under stabilizing selection. Evolution 64:763–774.

Guntrip, J., R. M. Sibly, and G. J. Holloway. 1997. The effect of novel environment and sex on the additive genetic variation and covariation in and between emergence body weight and development period in the cowpea weevil, *Callosobruchus maculatus* (Coleoptera, Bruchidae). Heredity 78:158–165.

Houle, D. 1989. The maintenance of polygenic variation in finite populations. Evolution 43:1767–1780.

Keightley, P. D., and W. G. Hill. 1989. Quantitative genetic variability maintained by mutation-stabilizing selection balance: sampling variation and response to subsequent directional selection. Genet. Res. 54:45–57.

Kingsolver, J. G., H. E. Hoekstra, J. M. Hoekstra, D. Berrigan, S. N. Vignieri, C. E. Hill, A. Hoang, P. Gibert, and P. Beerli. 2001. The strength of phenotypic selection in natural populations. Am. Nat. 157:245–261.

Kohn, L. A. P., and W. R. Atchley. 1988. How similar are genetic correlation structures? Data from mice and rats. Evolution 42: 467–481.

Kondrashov, A. S. 2003. Direct estimates of human per nucleotide mutation rates at 20 loci causing Mendelian diseases. Hum. Mutat. 21:12–27.

Lande, R. 1975. The maintenance of genetic variability by mutation in a polygenic character with linked loci. Genet. Res. 26: 221–235.

———. 1979. Quantitative genetic analysis of multivariate evolution, applied to brain:body size allometry. Evolution 33: 402–416.

———. 1980. Microevolution in relation to macroevolution. Paleobiology 6:233–238.

Lande, R., and S. J. Arnold. 1983. The measurement of selection on correlated characters. Evolution 37:1210–1226.

Lynch, M. 1988. The rate of polygenic mutation. Genet. Res. 51: 137–148.

Lynch, M., and B. Walsh. 1998. Genetics and analysis of quantitative traits. Sinauer, Sunderland, MA.

Paulsen, S. M. 1996. Quantitative genetics of the wing color pattern in the buckeye butterfly (*Precis coenia* and *Precis evarete*): evidence against the constancy of **G**. Evolution 50: 1585–1597.

Phillips, P. C., and S. J. Arnold. 1999. Hierarchical comparison of genetic variance-covariance matrices. I. Using the Flury hierarchy. Evolution 53:1506–1515.

Phillips, P. C., M. C. Whitlock, and K. Fowler. 2001. Inbreeding changes the shape of the genetic covariance matrix in *Drosophila melanogaster*. Genetics 158:1137–1145.

Platenkamp, G. A. J., and R. G. Shaw. 1992. Constraints on adaptive population differentiation in *Anthoxanthum odoratum*. Evolution 46:341–352.

Podolsky, R. H., R. G. Shaw, and F. H. Shaw. 1997. Population structure of morphological traits in *Clarkia dudleyana*. II. Constancy of within-population genetic variance. Evolution 51: 1785–1796.

Reeve, J. P. 2000. Predicting long-term response to selection. Genet. Res. 75:83–94.

Roff, D. A., and T. A. Mousseau. 1999. Does natural selection alter genetic architecture? An evaluation of quantitative genetic variation among population of *Allonemobius socius* and *A. fasciatus*. J. Evol. Biol. 12:361–369.

Roff, D. A., T. A. Mousseau, and D. J. Howard. 1999. Variation in genetic architecture of calling song among populations of *Allonemobius socius*, *A. fasciatus*, and a hybrid population: Drift or selection? Evolution 53:216–224.

Service, P. M. 2000. The genetic structure of female life history in *D. melanogaster*: comparisons among populations. Genet. Res. 75:153–166.

Shaw, F. H., R. G. Shaw, G. S. Wilkinson, and M. Turelli. 1995. Changes in genetic variances and covariances: **G** whiz! Evolution 45:143–151.

Shaw, R. G., and H. L. Billington. 1991. Comparison of variance components between two populations of *Holcus lanatus*: a reanalysis. Evolution 45:1287–1289.

Spitze, K., J. Burnson, and M. Lynch. 1991. The covariance structure of life-history characters in *Daphnia pulex*. Evolution 45: 1081–1090.

Steppan, S. J., P. C. Phillips, and D. Houle. 2002. Comparative quantitative genetics: evolution of the **G** matrix. Trends Ecol. Evol. 17:320–327.

Turelli, M. 1985. Effects of pleiotropy on predictions concerning mutation-selection balance for polygenic traits. Genetics 111: 165–195.

———. 1988. Phenotypic evolution, constant covariances, and the

maintenance of additive genetic variance. Evolution 42: 1342–1347.

Wagner, G. P. 1989. Multivariate mutation-selection balance with constrained pleiotropic effects. Genetics 122:223–234.

Wagner, G. P., G. Booth, and H. Bagheri-Chaichian. 1997. A population genetic theory of canalization. Evolution 51: 329–347.

Waldmann, P. A. S. 2000. Comparison of genetic (co)variance matrices within and between *Scabiosa canescens* and *S. columbaria*. J. Evol. Biol. 13:826–835.

Zeng, Z.-B. 1988. Long-term correlated response, interpopulation covariation, and interspecific allometry. Evolution 42: 363–374.

Corresponding Editor: D. Houle